An Analysis of Sierra Nevada Winter Orographic Storms: Ground-based Ice-Crystal Observations

BELAY B. DEMOZ,* RENYI ZHANG,† AND RICHARD L. PITTER

Desert Research Institute, Atmospheric Sciences Center, University of Nevada System, Reno, Nevada

(Manuscript received 6 July 1992, in final form 2 June 1993)

ABSTRACT

Systematic observations of the sizes, shapes, and degrees of riming of ice particles falling at a downwind station of a major mountain barrier are presented. The observational station was equipped to measure ice-particle masses from 1 μg to a few milligrams, and to measure ice-particle dimensions, habits, degrees of riming, and degrees of aggregation. The results are shown to be useful in learning where ice nucleation and growth take place in the cloud system.

The present study analyzed dissipating and developing winter orographic storm systems, which are representative of more than 60% of the storms observed over the study region. It suggests that most of the needles and columns observed at the ground may be formed by secondary ice production. Heavy riming was associated with light precipitation, while high precipitation rates were correlated with a high number fraction of aggregate crystals. Aggregation was found to be important in the process of precipitation development and the aggregate mass was mostly contained in the dendritic crystal growth region.

1. Introduction

During the 1986/87 season, an extensive field investigation of the winter storms that affected the central Sierra Nevada was done as part of the Sierra Cooperative Pilot Project (SCPP). Several investigators have reported on the evolution of supercooled water and mesoscale characteristics of the storms affecting this region (Reynolds and Kuciauskas 1988; Reynolds and Dennis 1986; Huggins and Rodi 1985; Huggins et al. 1990; Heggli and Rauber 1988; Heggli et al. 1983; Heggli and Reynolds 1985; Marwitz 1987; Deshler et al. 1990; Prasad 1986; Prasad et al. 1989; and references within). All the above authors concentrated on the characteristics of winter storms upwind of the main mountain crest of the Sierra Nevada. Only Huggins et al. (1990) addressed the downwind side by presenting, for the first time, a comparison of radiometric measurements of cloud liquid water made at Kingvale (KGV), California, and Truckee (TRK), California. KGV is located slightly west of the mountain crest at an elevation of 1857 m MSL and TRK is located in a downwind valley (Fig. 1). In their study, Huggins et al. did not present the microphysics of the storms.

The storms studied by SCPP, including the ones presented here, were classified into two main divisions by Heggli and Rauber (1988). The classification was based on the prevailing flow and resultant storm trajectory. The two divisions were of mainly zonal and meridional flow. Depending on the stage of development and mesoscale structure of the storms, the storms were further classified into occluding, dissipating, or developing type. A total of 63 storms were analyzed that affected the area from 1983/84 to 1986/87 winter field seasons. More than 60% of the storms studied were of the zonal type. The storms to be presented in the following sections belong to this group.

The Desert Research Institute (DRI) made ice-crystal observations at the ground west of the main Sierra crest as part of the SCPP investigations. The prime objective of the research was to develop a sampling and analysis technique for characterizing microphysical parameters of snowfall in preparation for studies to utilize these characteristics in assessing the effects of cloud seeding on microphysical processes and precipitation. The data presented here were collected from storms that affected this area on 18 and 22 December 1986 and 3 January 1987. The 18 and 22 December cases were characterized by a split flow in the middle troposphere associated with a dissipating storm, and the 3 January case was of a developing type embedded in strong westerly or southwesterly flow. A brief description of the synoptic structure of the storms is presented followed by a detailed discussion of the ground-

* Current affiliation: Institute for Environmental Studies, University of Illinois, Urbana, Illinois.

† Current affiliation: Department of Earth, Atmospheric, and Planetary Sciences, Massachusetts Institute of Technology, Cambridge, Massachusetts.

Corresponding author address: Dr. Belay B. Demoz, Institute for Environmental Studies, University of Illinois, Room 352, 1101 West Peabody Drive, Urbana, IL 61801-4723.

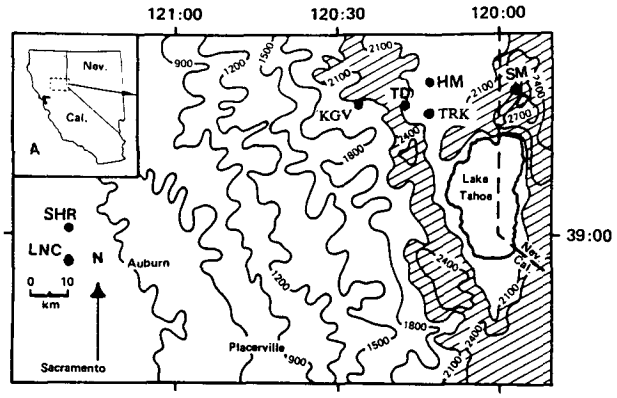

FIG. 1. Location and elevation (m) contour of the sampling area showing sampling and instrumentation stations. Kingvale (KGV), Truckee (TRK), Tahoe Donner (TD), Hobbart Mills (HM), Slide Mountain (SM), Sheridan (SHR), and Lincoln (LNC) are shown on the figure.

based ice-crystal and snowflake observations. Since the synoptic structure of these storms was reported as part of SCPP, much attention is given here to the microphysics analysis.

This paper investigates ice-phase processes of clouds based on a systematic analysis of the ground-observed ice crystals and snowflakes from storms that affected the central Sierra Nevada in the winter of 1986/87. The results give insight into how riming, aggregation, and ice-crystal fragmentation act and interact in Sierra Nevada winter storms.

2. Research site and procedure

The ground ice-crystal sampling site was located about 9 km east of the Sierra Nevada crest line, at an elevation of 2100 m. The local topography of this area is presented in Fig. 1. The site, Tahoe Donner (TD), was located at the edge of a clearing among conifer trees, providing unobstructed snowflake paths to the collection point while buffering against strong winds and blowing snow.

Snow crystals were collected at the ground station using a 2.5-cm-radius dish. The petri dish was exposed in a horizontal position for 3–60 s, depending on the concentration of falling snow. Care was exercised to prevent the contamination of the samples by blowing snow. Exposure times were varied to get a representative sample, and yet to minimize the overlap of crystals on the dish. During the storm, samples were taken at 10-min intervals, and two photographs were taken through a microscope at 20× magnification. The first photograph showed the snowflakes and the second showed the freshly melted drops. Photography was performed using a 35-mm SLR camera mounted on the microscope.

Subsequent analysis of the photographic data was made by projecting the slides with a magnification of 117× onto a screen. Ice crystals were classified according to the Magono and Lee (1966) classification scheme. The mass of each ice crystal was calculated from the melted drop photographs by noting that the drops were hemispherical in shape (Mitchell et al. 1990).

For each ice crystal, a confidence factor varying from 1 to 4 was given. The highest confidence of 1 was given to shapes for which the particle type could be unquestionably identified, while higher values indicated lower confidence in the classification of the ice particles. In the present study, only snow crystals with confidence factors between 1 and 3 were included in the analysis. The shape classification allows characterization of rimed crystals, aggregates, and obvious crystal fragments.

Microwave radiometer measurements of integrated liquid water and wind information were also routinely recorded at the TRK and Slide Mountain (SM), Nevada, weather stations. These data, together with the synoptic charts, were used to locate frontal passage across the sampling station. During the SCPP seasons, radar and sounding data were taken on the upwind side of the crest at Sheridan (SHR), California. A complete summary of the instrumentation used in SCPP was presented by Reynolds and Dennis (1986).

3. Results

a. Experimental conditions

1) THE STORM OF 18–19 DECEMBER 1986

A short wave approached the West Coast on 18 December 1986. At 1200 UTC (all times are in UTC), the low pressure was located off the Washington State coast while a high pressure center was over Idaho. The surface cold front at this time (1200) stretched from about 50° to about 34°N and curved southwest into the Pacific Ocean (Fig. 2a). The relative location of the high and low pressure centers, as observed on 500-mb charts, caused the flow to split (Heggli and Rauber 1988) over the central Sierra Nevada.

The wind speed and direction measurements at SM are presented in Fig. 2b. As the low pressure center moved east, the wind direction at the sampling site was mostly from the southwest (about 240°) and wind speed showed a marked increase. The wind direction, predominantly from 250°, stayed the same even after the frontal passage. The front passed KGV about 0000, 19 December and SM between 0100 and 0300 (UTC) the same day. The cross-barrier nature of the wind (and the relatively strong wind speeds) was considered good for orographic lifting and liquid water development. The slow and dissipating nature of the front did not allow for wind measurements to pinpoint the location of exact time of the frontal passage. Contour plots of soundings made at KGV (Hemmer et al. 1987) did not show strong thermal discontinuity, mainly due to

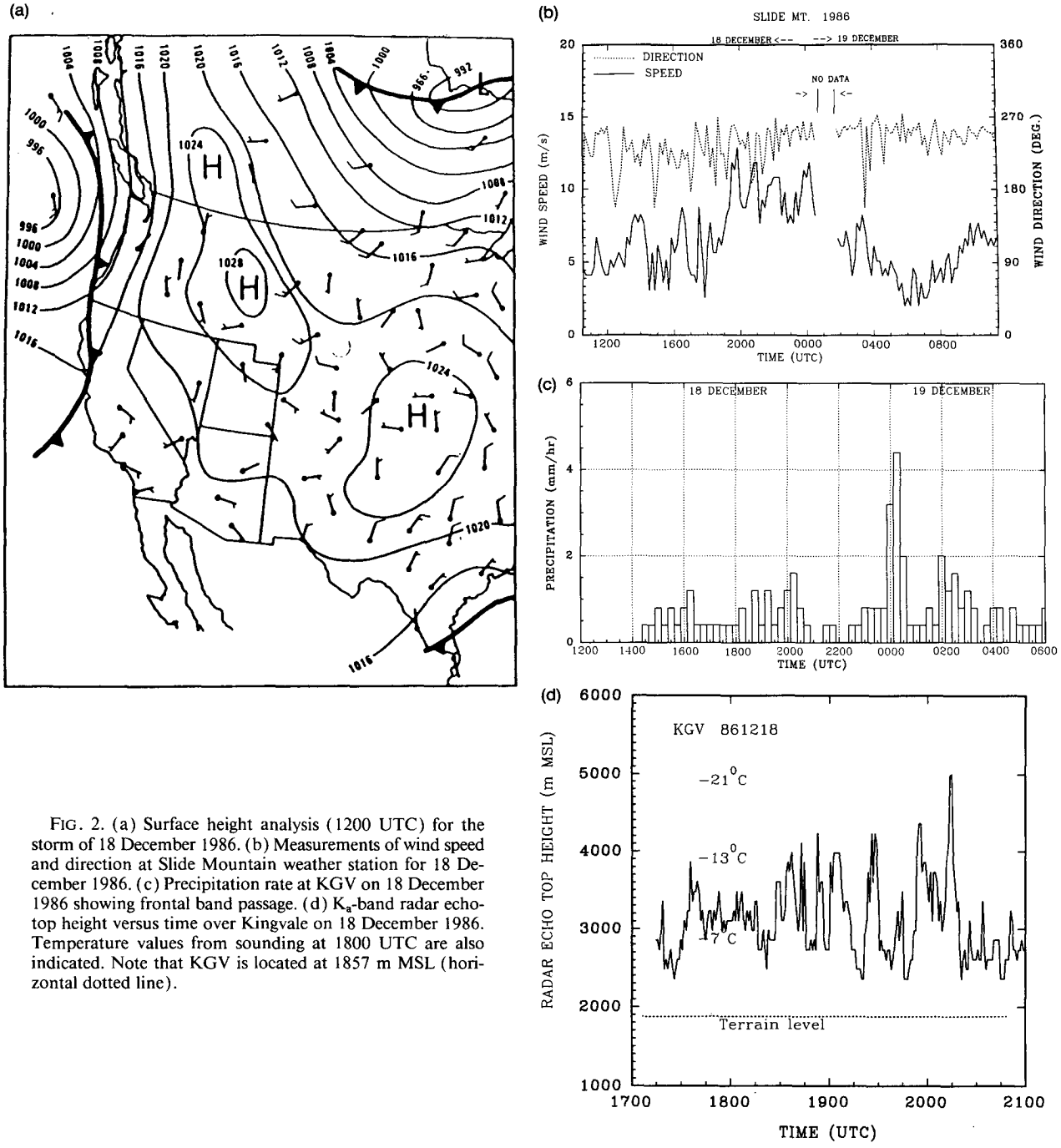

FIG. 2. (a) Surface height analysis (1200 UTC) for the storm of 18 December 1986. (b) Measurements of wind speed and direction at Slide Mountain weather station for 18 December 1986. (c) Precipitation rate at KGV on 18 December 1986 showing frontal band passage. (d) K_a-band radar echo-top height versus time over Kingvale on 18 December 1986. Temperature values from sounding at 1800 UTC are also indicated. Note that KGV is located at 1857 m MSL (horizontal dotted line).

the weakness of the frontal organization of the storm. But the precipitation record at KGV, given in Fig. 2c, indicated the frontal passage to be between 0000 and 0100.

At KGV, a K_a-band radar was operated by DRI. A plot of the radar echo-top height versus time is given in Fig. 2d. It shows that cloud depth was generally between 1 and 2 km before frontal passage and cloud-top temperatures were warmer than −20°C. Note that KGV is located at an altitude of 1857 m MSL.

This storm was seeded from aircraft with AgI between 1841 and 1857 (Deshler et al. 1990). The fixed target for the experiment was KGV, which is located more than 20 km west of TD, the ground sampling station for the ice-crystal data discussed here. Deshler et al. (1990) presented a detailed analysis of the effect of seeding this storm. According to the report, they were unable to determine "for certain" seeding effects from ground-measured observations. As a result, and since the seeding window (about 16 minutes) was small

compared to the storm duration, seeding effects are not discussed here. It is assumed that the effect, if any, is negligible. The reader is referred to Deshler et al. (1990) for a discussion of seeding effects and radar analysis of this storm.

2) THE STORM OF 22–23 DECEMBER 1986

The general synoptic-scale structure of the storm and its classification is similar to the storm of 18 December 1986 discussed above. The surface height analysis map at 1200 UTC, SM wind records, and precipitation rate at KGV are given in Figs. 3a, 3b, and 3c, respectively. The surface front passed KGV at 1700, 22 December and was distinguished by a single, frontal precipitation band. An orographic cloud remained for several hours after the frontal passage over the Sierra Nevada and produced some precipitation. K_a-band radar data for this day starts at 1724, which was after the ground sampling at TD stopped, and is not presented here. However, it indicated that cloud-top temperatures were −20°C or warmer at an altitude of less than about 6 km. According to Heggli and Rauber (1988), the clouds were stratus deck, 1.5–2 km thick. An extended discussion of the classification of the storm system was reported by Heggli and Rauber (1988) and its radar analysis by Huggins et al. (1990).

Winds at SM showed a constant direction but decreasing speed until 0300 UTC 23 December. At 0300, the wind direction changed from westerly to northerly and northeasterly, accompanied by a slight increase in speed. This change in speed and direction was associated with the intensification of the high pressure center located at eastern Nevada and the weakening of the storm. The passage of the front at SM, after 1700 (between 1900 and 2000 UTC), was accompanied by a slight leveling off of the speed but no change in direction.

3) THE STORM OF 3–4 JANUARY 1987

The data collected during this storm is documented by Hemmer et al. (1987). The surface analysis map at 1200, SM wind record, and precipitation rate and radar data at KGV are given in Figs. 4a, 4b, and 4c, respectively. Surface and 500-mb chart analysis by Hemmer et al. (1987) showed a low center approaching the sampling area with a southwesterly flow. The front passed KGV after 0000 UTC January based on data from sounding contours as a drop in the moisture level and temperature values. Most of the precipitation that fell on this day was from prefrontal clouds. Soundings and radar plots indicated that temperatures at echo-top heights were −18°C or colder. The SM wind ob-

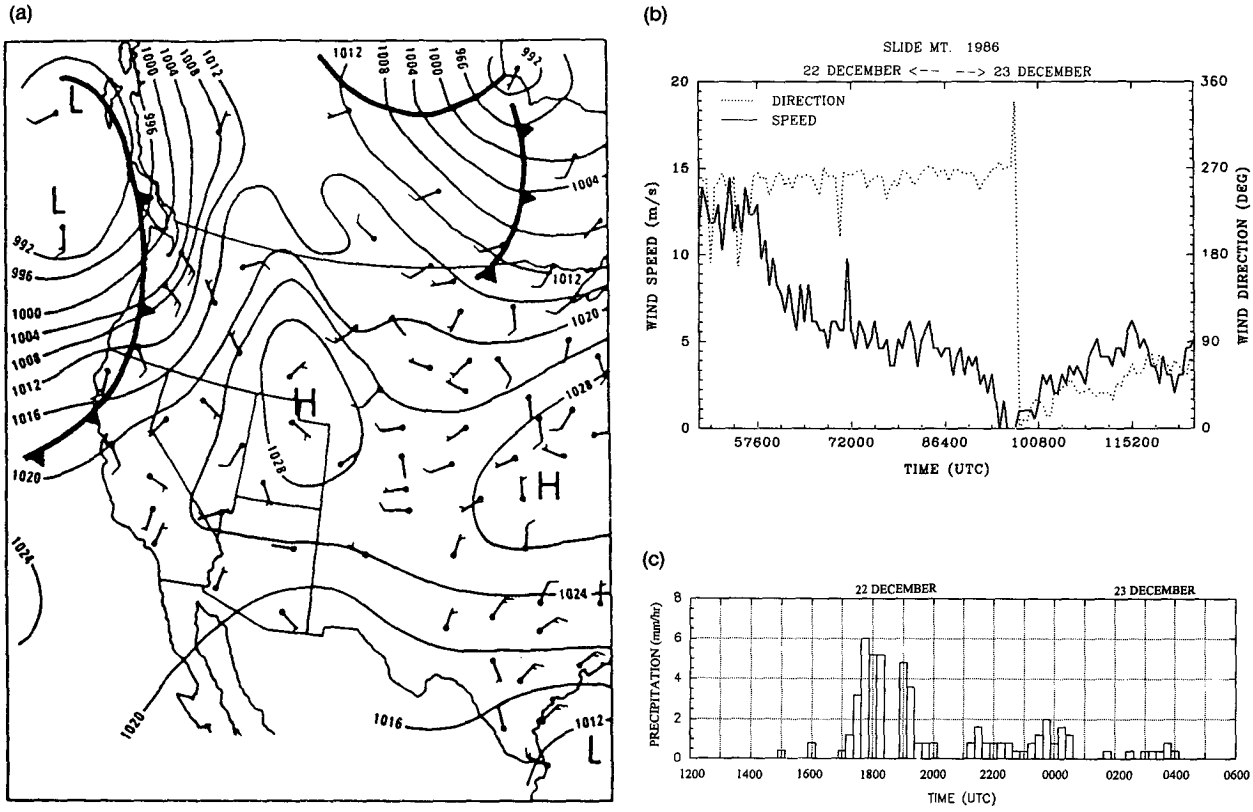

FIG. 3. (a) Surface height analysis (1200 UTC) for the storm of 22 December 1986. (b) Measurements of wind speed and direction at Slide Mountain weather station for 22 December 1986. (c) Precipitation rate at KGV on 22 December 1986 showing frontal band passage.

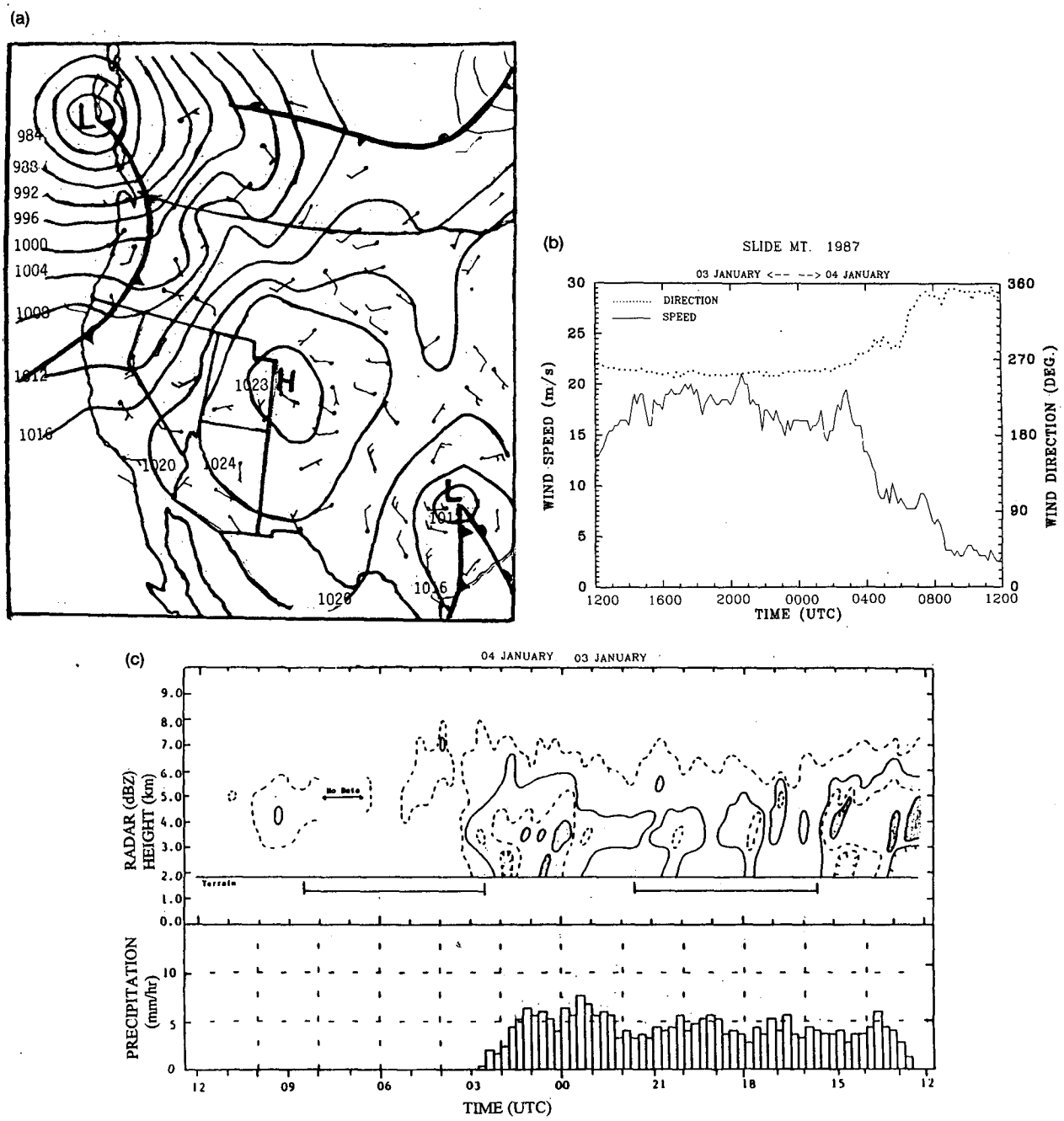

FIG. 4. (a) Surface height analysis (1200 UTC) for the storm of 3 January 1987. (b) Measurements of wind speed and direction at Slide Mountain weather station for 3 January 1987. (c) Precipitation rate and time–height plot of radar data over KGV (top), and precipitation rate at KGV on 3 January 1987 (bottom). Radar data are contoured in 5-dBZ increments beginning with 10 dBZ, from Hemmer et al. (1987).

servations indicate that the ice-crystal sampling station was under postfrontal cloud influence after 0000 UTC 4 January.

b. Ice-crystal and snowflake observations

Figure 5 shows the contribution of a given ice particle of less than a particular mass to the total snow mass of a storm, broken into total snowfall, and the contribution due to rimed, aggregated, and fragmented ice particles. The three plots correspond to storms on 3 January 1987 (Fig. 5a), 22 December 1986 (Fig. 5b), and 18 December 1986 (Fig. 5c). The figure shows that the contribution of aggregation to the snowfall was much larger than that of rimed and fragmented ice crystals combined for the 3 January case. For the

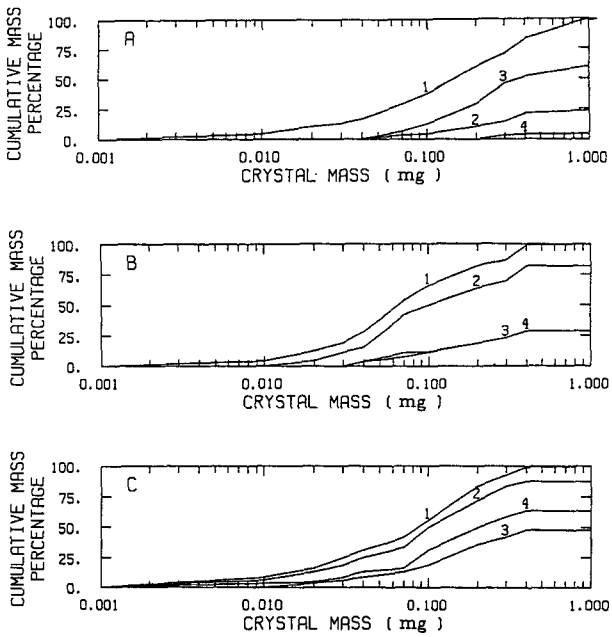

FIG. 5. Cumulative mass percentage for overall storm as a function of crystal mass: total snowfall—1, riming—2, aggregation—3, and crystal fragmentation—4 for (a) 3 January, (b) 22 December, and (c) 18 December.

18 and 22 December cases, the contribution was mostly from rimed crystals even though aggregation was observed. This is a direct reflection of the liquid water available in the storms as we will elaborate upon below.

The time series of microphysical properties of the 3 January 1987 storm is presented in Fig. 6. It shows how the ice-particle number percentage varied with time during the storm. For example, in Fig. 6a, the initial high number concentration of warm column habit crystals (N1a, N1b, N1c, N1e, N2a, N2c) and planar crystals (P1a, P1b, P1c, P1e, P2a, P2c, P2f, P7a) gave way to higher concentration of cold habit crystals (C1c, C2a, C2b, S1, S3) following the passage of the surface front about to 0100 UTC. The virtual absence of heavily rimed particles like R3b and R4b indicates that the ice crystals were unrimed after frontal passage. The precipitation and temperature records at TD during this time are also shown in Fig. 6e. It shows that the cold habit crystals dominated starting at 0000 when the frontal precipitation band appeared. On this day, aggregates and fragmented crystals were observed throughout the sampling time while riming stopped or was at a minimum after the frontal passage.

Similarly, the time series of the microphysical properties of the 18 and 22 December storms is presented in Figs. 7 and 8. In these figures, heavily rimed (R2b, R3b, R4b), warm habit (N1a, N1e and N2c), planar or dendritic (P1a, P1e, P2f, P7a), and miscellaneous ice crystals (I4) are presented. The surface temperature at TD during the observation period for these two storm days was constant and slightly below 0°C.

Mass percentages of the observed ice particle types found in rimed crystal habits for 18 and 22 December 1986 cases are presented in Table 1. Table 2 lists the mass percentage of the observed crystal types found in aggregates for 3 January 1987. In Table 3, a summary of the habits of 1083 crystals photographed at TD during the 1986/87 winter field season is given. In the tables, aggregates are classified by the habit of their major component while fragments are classified by their parent crystal habit.

The integrated liquid water (mm) through the depth of the atmosphere is given in Figs. 9, 10, and 11 for the storms studied. The liquid water and vapor values were measured by a dual-channel microwave radiometer (Guirand et al. 1979) located at TRK. The data used for these plots are averaged every 15 min.

4. Discussion

a. Ice-crystal habits

The habits of falling ice crystals varied dramatically from storm to storm, and within a single storm before

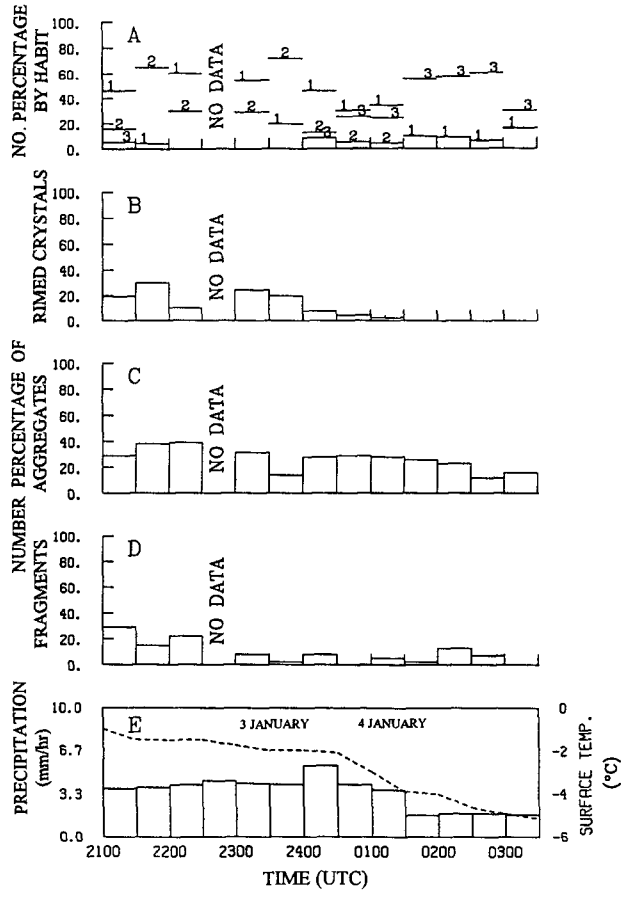

FIG. 6. Time series of the ground-observed microphysical properties for the 3 January 1987 storm. The numbers 1, 2, and 3 represent planar or dendritic, warm and cold habit crystals, respectively.

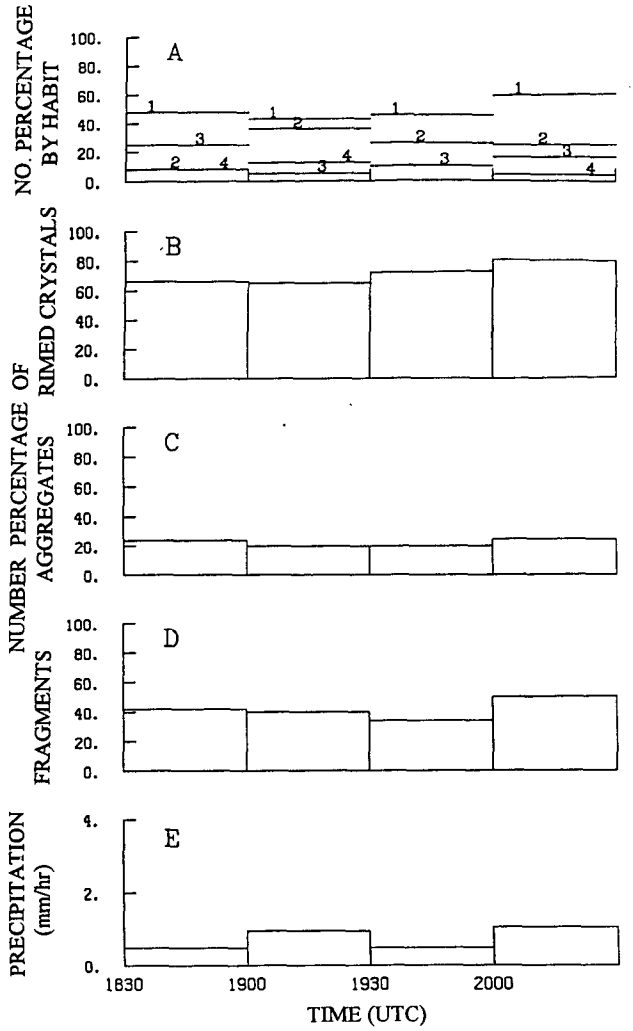

FIG. 7. Time series of the ground-observed microphysical properties for the 18 December 1986 storm. The numbers 1, 2, 3, and 4 represent heavily rimed, warm, planar or dendritic, and miscellaneous (I4) habit crystals, respectively.

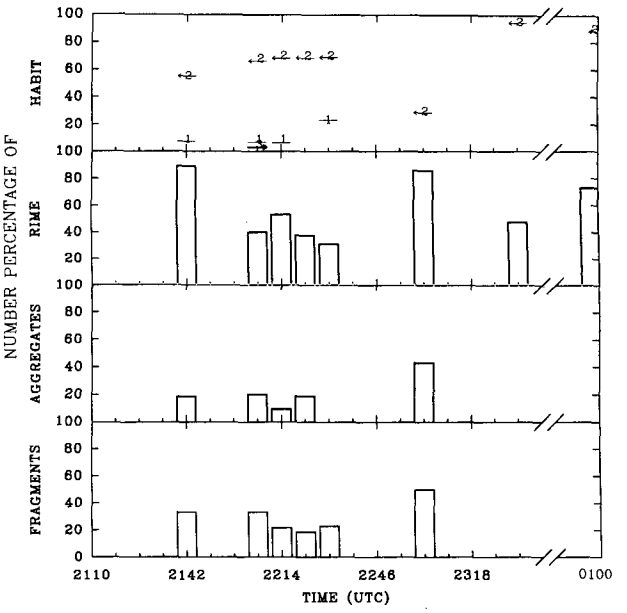

FIG. 8. Time series of the ground-observed microphysical properties for the 22 December 1986 storm. The numbers 1, 2, and 3 represent planar or dendritic, warm, and cold habit crystals, respectively.

and after the surface frontal passage. These habits are believed to reflect the temperature and moisture conditions within the cloud where ice crystals grew. In the first two storms, 18 and 22 December 1986, the ice crystals were heavily rimed, but relatively few aggregated; in the 3 January 1987 storm, the crystals were lightly rimed, but many aggregated. The differences in ground-observed ice-crystal habit also reflected the synoptically different nature of the storms. The integrated liquid water for the December storms was generally greater than 0.1 mm, while for the January case study it was less than 0.1 mm during the sampling hours. The 18 and 22 December cases were dissipating storm types while the 3 January 1987 case was a developing storm embedded in strong westerly flow.

Dendritic crystals, radiating assemblages of plates, and side planes were common habits in these storms. They constituted 12%, 13%, and 18% of the crystals observed (Table 3), respectively, and were often found in aggregates. Planar dendrites were also frequently observed to be rimed. The cold habits, consisting of short columns and bullets, comprised about 6% of the total number of crystals sampled, while long columns and needles made about 28%. The habits were observed to change during the storm, with warm habits more prevalent at the beginning of a storm and cold temperature habits more prevalent at the trailing edge of the storm (Fig. 6a).

The temperature changes associated with the passage of the cold front at the surface were at times very weak. But as the January case study shows, they were generally reflected by changes in both ice-crystal habits and the degree of riming (Figs. 6a and 6b). After passage of the cold front, the number fractions of cold types of crystals such as side planes, bullets, and short

TABLE 1. Mass percentage of observed crystal types found in the rimed particles for 18 and 22 December storms.

Storm date	Crystal type	Mass percent
18 December 1986	Warm habit (N1a, N1e, N2c)	2.4
	Heavily rimed dendritic (R3b)	85
	Others (I4, R2b, R4b)	12.6
	Total	100
22 December 1986	Warm habit (N1a, N1e, N2c)	27
	Heavily rimed dendritic (R3b)	71
	Others (I4, R2b)	2
	Total	100

TABLE 2. Mass percentage of observed ice-particle types found in aggregates for the 3 January 1987 storm.

Crystal type	Mass percent
Warm habit (N1c, N1e, N2c)	9
Dendritic/planar (P1a, P1b, P1c, P1e, P2a, P2c, P2f, P7a)	55
Side planes (S1, S3)	34
Cold column (C1c, C2a, C2b)	2
Total	100

columns increased and subsequently remained high. Similarly, there was a notable decrease in the number fraction of rimed crystals after the cold-frontal passage, which may be associated with the relative decrease of liquid water after the frontal passage. The bulk of the liquid water in the Sierra Nevada winter storms is located between about 0° and −10°C as observed by Gordon and Marwitz (1986), Heggli et al. (1983), Heggli and Rauber (1988), Warburton and DeFelice (1986), and others. In this temperature range over this area, dendritic crystals much larger than the size required for the onset of riming were observed from aircraft investigations of the 18 December 1986 storm by Deshler et al. (1990). They found dendrites of 300-μm size at the −13°C level. From the work of Reinking (1979), dendritic crystals must be about 300 μm in size for riming to commence. This suggests that the degree of riming observed at the ground reflects the liquid water available below the −13°C level.

b. *Characteristics of aggregation*

Aggregation of ice crystals is an important mechanism for particle growth to precipitation size. In our studies, the contribution of aggregates to the total snowfall mass was always significant. Much previous work has been conducted on the process of aggregation, including Sasyo (1971), Jiusto (1971), Hobbs et al. (1974), Rauber (1987), Prasad (1986), Prasad et al. (1989), and Mitchell (1988, 1991). Hobbs et al. (1974) discussed the factors that affected aggregation. They concluded that the probability of the occurrence of aggregation generally decreases with decreasing temperature, with a local peak in the dendritic growth region. A similar result was also reported by Prasad et al. (1989). Rauber (1987) showed that the primary components of aggregation were found to be planar dendrites. His results minimized the importance of warm temperatures on aggregation, as does the present study.

In the present study, the primary components of aggregates were planar dendrites, radiating assemblages of plates, and side planes (Table 2). The present results revealed that 55% of the total aggregate mass was contained in those aggregates whose main habits indicated temperatures in the dendritic growth region, approximately between −10° and −20°C. Many of these aggregates contained a large, centrally located crystal. This suggests that the initiation of aggregation requires some sort of a larger crystal capable of falling through a cloud containing smaller crystals and collecting some of the smaller crystals it interacts with.

TABLE 3. Ice-crystal habit analysis.

Crystal habit	Number of crystals	Percent of sample
Dendritic/planar (P1a, P1b, P1c, P1e, P2a, P2f)	129	12
Radiating assemblage of plates (P7a)	138	13
Short columns and bullets (C1c, C1e, C2a, C2b)	68	6
Long columns and needles (N1a, N1b, N1e, N2a, N2c)	312	28
Heavily rimed (R2b, R3b, R4b)	149	14
Side planes (S1, S2, S3)	193	18
Irregular (I4)	94	9
Total	1083	100

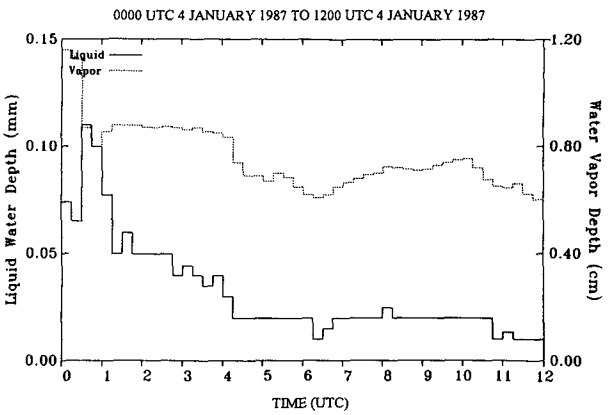

FIG. 9. Radiometer-measured liquid water and water vapor at Truckee for 3 January 1987. The plot shows 15-min average data.

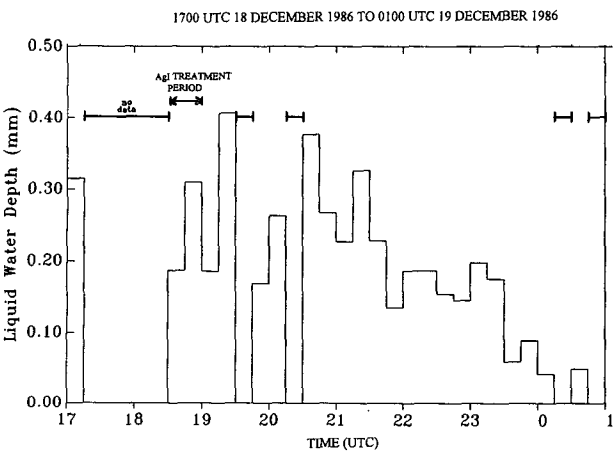

FIG. 10. Radiometer-measured liquid water at Truckee for the 18 December 1986 storm.

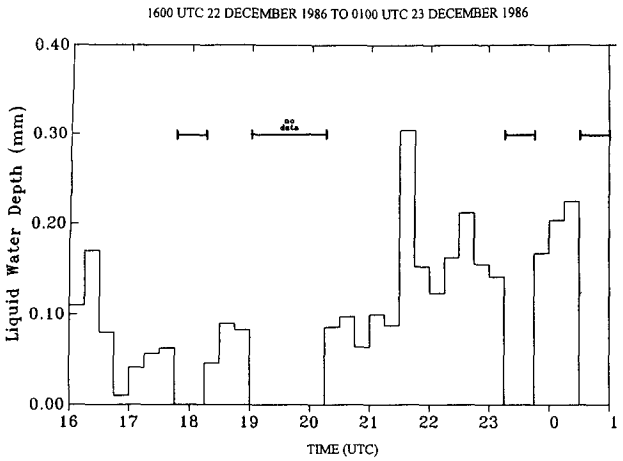

FIG. 11. Same as Fig. 10 but for 22 December 1986.

Side planes were also commonly found in aggregates (about 34%). As suggested by Furukawa and Kobayashi (1978), those ice crystals are polycrystalline, possibly nucleated by cloud droplets freezing at temperatures colder than −20°C. Side planes were usually associated with aggregates and arrived at the ground after the cold frontal passage with little riming. Because of their sizes and protruding arms, side planes were effective for aggregation.

Warm columnar and needle aggregates were also found, although their mass seldom exceeded 10% of the total aggregate mass. These aggregates were generally found in the early periods of the storm, when the surface temperature was close to 0°C.

Simultaneous riming and aggregation were observed most of the time during the sampling periods. The amount of riming associated with aggregation could be divided into two categories. Heavy riming, as that of 18 and 22 December, often accompanied by graupel, was associated with convective activity. During periods of heavy riming, both the precipitation rate and the amount of aggregation present were diminished (Fig. 7). In contrast, situations with a higher percentage of aggregates were characterized by moderate or light riming (Fig. 6). Light riming did not appear to inhibit aggregation.

On 3 January 1987, the observations show 63% of the total mass was produced by aggregation (Fig. 5a). On the same day, the surface temperature was between 0° and −5°C, which indicates that the temperatures were much colder higher in the clouds where aggregation took place. The surface temperature was at its coldest after the cold-frontal passage, and aggregation was still dominant. This indicates that a "warm layer" on the ice crystals, as suggested by Hobbs et al. (1974) and many others, may not be necessary for aggregation to occur. This observation supports the argument reported by Rauber (1987) and the findings of Mitchell (1988).

A higher precipitation rate was often associated with the occurrence of heavy aggregation. The correlation between aggregation and precipitation rate was most notable in the 3 January storm case.

c. *Characteristics of riming*

Table 1 indicates that about 85% and 71% of the rimed masses were associated with planar crystals, principally dendrites, for the two 1986 storms, respectively. For a dendritic crystal, the collecting area is larger and the collection efficiency is also higher since the dendrites act somewhat like a filter, collecting drops attempting to flow between its branches. This "filter" effect was found to increase the collision efficiency by up to an order magnitude greater than that of a nonporous crystal of the same size (Lew et al. 1986).

Warm habits also rime to a degree, which is to be expected in Sierra Nevada winter storms, since most of the supercooled liquid water in the cloud is present at temperatures between −8° and −10°C as noted earlier. Conversely, the short columns and bullets (< −20°C) exhibited very little riming during the days sampled. This may be due to their origination and growth in regions behind the surface cold front, where the cloud was characterized by low liquid water content. The cold habit crystals usually appeared after the frontal passage, when there were often lower amounts of supercooled liquid water in the clouds, as the microwave radiometer measurements in Figs. 9–11 show to be the case. The 3 January case (Fig. 9) data start from 0000 and cover observations of the liquid water from postfrontal clouds. The data show a sharp drop of values to lower than 0.05 mm. At this time, cold habit crystals and almost no riming were observed. Recall from Fig. 5 that most of the snowfall contribution came from aggregates and very little from riming or fragmentation. For the 18 and 22 December case studies, Figs. 10 and 11, respectively, riming was more important than aggregation and fragments for the total snowfall. This suggests that the liquid water available in the clouds was higher than the 3 January case study; a comparison of the entire storm liquid water was not possible due to contaminated data during the pre-cold-frontal period on the January case study. As deduced from the microphysics data independently, the 18 December case was also the storm that showed large liquid water values relative to the other cases.

Heavy riming cases were usually associated with low precipitation rates (Fig. 7), which reflect a relatively small number concentration of ice crystals within the cloud. This does not agree with observations made in the upwind side of the Sierra Nevada and those made by Feng and Grant (1982). Feng and Grant (1982) reported an increase in riming associated with heavy precipitation in the Front Range in Colorado. Perhaps this is because our site is downwind of the barrier. Observations similar to ours were reported in the Cascades

by Hobbs (1975). On 18 and 22 December 1986, 82% and 90%, respectively of the total snowfall masses were associated with heavy riming (Figs. 5a and 5c). During these observation periods, the precipitation rates were less than 2 mm h^{-1}, even though the liquid water measured by radiometer during those storm days was much higher than the 3 January case study (during the period when data were available).

Riming and fragmentation were found to be correlated in the overall storm mass (Fig. 5). A similar result was also reported by Vardiman (1978). This may have been the result of large fall speeds of rimed ice particles increasing the rate of fragmentation of dendritic branches by collisions of rimed and unrimed ice particles. Previous observations showed that fall speeds of unrimed dendrites were usually between 30 and 60 cm s^{-1} (Davis 1974), and the fall speeds for rimed dendrites varied between 80 and 160 cm s^{-1} (Locatelli and Hobbs 1974).

Rauber (1987) found that if the echo tops were warmer than −20°C, the warm habits constituted less than 2% of the total ice-crystal population. He assumed that this indicated an inefficient nucleation at temperatures greater than −10°C and inactivity of the Hallett–Mossop rime-splintering mechanism of ice-crystal multiplication (Hallett and Mossop 1974).

In contrast, larger quantities of warm habits are found in the present study. During the 18 December storm, between 30% and 40% of the total snow mass was associated with ice crystals in the warm column region, despite their individually small masses. Similarly, during the 22 December case, a large percentage of the ice crystals were warm habit. The virtual absence of cold habit indicated that the cloud top was warmer than −20°C. Soundings made at KGV together with echo-top height measurements from a vertically pointed K_a-band radar revealed that the cloud tops for 18 and 22 December cases were warmer than −20°C. Often, high concentration of these warm habit crystals was accompanied by higher riming rate. It was shown that the rate of riming was well correlated with the warm habit crystals (Figs. 6a and 6b). We therefore postulate that the high concentration of warm column and needle habits observed were due to secondary ice formation.

5. Summary and conclusions

An observational study has been conducted of the ground microphysical characteristics of storms over the Sierra Nevada from a high-altitude station located on the downwind side of the barrier. The case studies presented were selected from the 1986/87 winter season. The results of this study are summarized below.

This study found that the habits of ice crystals varied between storms and changed during the cold-frontal passage of a storm. The habits reflect the temperature and moisture conditions of the ice-crystal growth region. The ice-crystal habits from the dissipating and developing case studies were also different with less riming observed in the latter storm types. Larger amounts of warm habits and rime crystals were observed prior to surface cold-frontal passage. The integrated liquid water measurements made during these storms confirm the conclusions made from the ground ice-crystal observations. Since the data presented in this work does not cover the entire storm duration, the points made here need to be investigated further.

Contribution of aggregation to the total snowfall mass was significant. Most of the aggregate mass was contained in the dendritic crystal growth region. Both aggregation and riming were observed simultaneously through most of the storm's duration, and when riming was heavy, aggregation and precipitation were both diminished. On the other hand, periods of heavy aggregation were associated with high precipitation. This work supports that a "warm layer" is not necessary for aggregation to occur. Planar dendrites, radiating assemblage of plates, and single planes were observed to be the primary components of crystal aggregates.

Cold habit crystals, such as side planes, short columns, and bullets, were usually observed after surface cold-frontal passage and were less likely to be rimed. These findings are consistent, for most storms, with the lower postfrontal values of observations of liquid water determined by the dual-channel microwave radiometer. The observation of riming on most of the dendritic crystals suggests that the bulk of the liquid water was located below their diffusional growth region (about the −13°C level). Riming and fragmentation of crystals were found to be correlated. At the same time, a high concentration of warm habit crystals was accompanied by a higher riming rate. These and the fact that cloud tops were warmer than −20°C leads to the conclusion that most of the warm column and needle crystals observed were formed by secondary ice formation.

This paper has presented a systematic use of ground-observed ice-crystal habits to gain insight into cloud microphysical processes. An attempt has been made to qualitatively explain how riming, aggregation, and ice-crystal fragmentation act and interact in different types of winter storms that affect the Sierra Nevada. We have also attempted to support our conclusions with synoptic and radar measurements. Even though a majority of the storms over this area since the 1983/84 winter season are of the same classifications as the ones presented here, more case studies and complete storm sampling are needed to accurately characterize the winter orographic snowfall over this region.

Acknowledgments. We would like to acknowledge Dr. Steven Chai, Mr. Arlen Huggins, and Mr. Dave Mitchell of the DRI and the anonymous reviewers for their comments and discussions. This research was conducted under the sponsorship of the National

Oceanic and Atmospheric Administration (NOAA), in collaboration with the Sierra Cooperative Pilot Program (SCPP), sponsored by the U.S. Bureau of Reclamation.

REFERENCE

Davis, C. I., 1974: Ice nucleating characteristics of various AgI aerosols. Ph.D. dissertation, University of Wyoming, 259 pp. [Available from the Department of Atmospheric Sciences, University of Wyoming, WY 82071.]

Deshler, T., D. W. Reynolds, and A. W. Huggins, 1990: Physical response of winter orographic clouds over the Sierra Nevada to airborne seeding using dry ice or silver iodide. *J. Appl. Meteor.*, **29,** 288–330.

Feng, D., and L. O. Grant, 1982: Correlation of snow crystal habit, number flux and snowfall intensity from ground observations. Preprints, *Conf. on Cloud Physics,* Chicago, IL, Amer. Meteor. Soc., 485–487.

Furukawa, Y., and T. Kobayashi, 1978: On the growth mechanism of polycrystalline snow crystals with a specific grain boundary. *J. Cryst. Growth,* **45,** 57–65.

Gordon, G. L., and J. D. Marwitz, 1986: Hydrometer evolution in rainbands over the California valley. *J. Atmos. Sci.*, **43,** 1087–1100.

Guirand, F. D., J. Howard, and D. C. Hogg, 1979: A dual-channel microwave radiometer for measurement of precipitable water vapor and liquid. *IEEE Trans. Geosci. Elec.*, **GE-17,** 129–136.

Hallett, J., and S. C. Mossop, 1974: Production of secondary ice particles during the riming process. *Nature,* **249,** 26–28.

Heggli, M. F., and D. W. Reynolds, 1985: Radiometric observations of supercooled liquid water within a split front over the Sierra Nevada. *J. Climate Appl. Meteor.*, **24,** 1258–1261.

——, and R. M. Rauber, 1988: Characteristics and evolution of supercooled water in wintertime storms over the Sierra Nevada: A summary of microwave radiometric measurements taken during the Sierra Cooperative Pilot Project. *J. Appl. Meteor.*, **27,** 989–1015.

——, L. Vardiman, R. E. Stewart, and A. W. Huggins, 1983: Supercooled liquid water and ice crystal distributions within Sierra Nevada winter storms. *J. Climate Appl. Meteor.*, **22,** 1875–1886.

Hemmer, G. L., R. M. Rauber, A. W. Huggins, T. F. Lee, A. P. Kuciauskas, C. J. Wilcox, and R. D. Elliot, 1987: SCPP meteorological and statistical support, interim progress Rep. 1986–1987. [Available from Bureau of Reclamation, Division of Atmospheric Resources Research, D-1220, Denver Federal Center, Denver, CO 80225.]

Hobbs, P. V. 1975: The nature of winter clouds and precipitation in the Cascade Mountains and their modification by artificial seeding. Part I: Natural conditions. *J. Appl. Meteor.*, **14,** 783–804.

——, S. Chang, and J. D. Locatelli, 1974: The dimensions and aggregation of ice crystals in natural clouds. *J. Geophys. Res.*, **79,** 2199–2206.

Huggins, A. W., and A. R. Rodi, 1985: Physical response of convective clouds over the Sierra Nevada to seeding with dry ice. *J. Climate Appl. Meteor.*, **24,** 1082–1098.

——, R. J. Meitin, and R. F. Reinking, 1990: Comparison of radiometric measurements of cloud liquid water near a mountain crest and over a downwind valley. *Proc. Fifth Conf. on Mountain Meteorology,* Boulder, CO.

Jiusto, J., 1971: Crystal development and glaciation of a supercooled cloud. *J. Rech. Atmos.*, **5,** 69–85.

Lew, J. K., D. C. Montague, and H. R. Pruppacher, 1986: A wind tunnel investigation on the riming of snowflakes. Part II: Natural and synthetic aggregates. *J. Atmos. Sci.*, **43,** 2410–2417.

Locatelli, J. D., and P. V. Hobbs, 1974: Fall speeds and masses of solid precipitation particles. *J. Geophys. Res.*, **79,** 2185–2197.

Magono, C. and C. W. Lee, 1966: Meteorological classification of natural snow crystals. *J. Fac. Sci.,* Ser. 7, **2,** 321–362.

Marwitz, J. D., 1987: Deep orographic storms over the Sierra Nevada. Part I: Thermodynamic and kinematic structure. *J. Atmos. Sci.*, **44,** 159–173.

Mitchell, D. L., 1988: Evolution of snow-size spectra in cyclonic storms. Part I: Snow growth by vapor deposition and aggregation. *J. Atmos. Sci.*, **45,** 3431–3451.

——, 1991: Evolution of snow-size spectra in cyclonic storms. Part II: Deviation from the exponential form. *J. Atmos. Sci.*, **48,** 1885–1899.

——, R. Zhang, and R. L. Pitter, 1990: Mass–dimension relationships for ice particles and the influence of riming on snowfall rates. *J. Appl. Meteor.*, **29,** 153–163.

Prasad, N., 1986: Precipitation development in seeded clouds over the Sierra Nevada. Report #A5152, Department of Atmospheric Sciences, University of Wyoming, Laramie, WY 82071. Contract 2-07-81-VO256, Bureau of Reclamation. [Available from Bureau of Reclamation, Division Atmospheric Resources Research, D-1220, Denver Federal Center, Denver, CO 80225.]

——, A. R. Rodi, and A. J. Heymsfield, 1989: Observational and numerical simulations of precipitation development in seeded clouds over the Sierra Nevada. *J. Appl. Meteor.*, **28,** 1031–1049.

Rauber, R. M., 1987: Characteristics of cloud ice and precipitation during wintertime storms over the mountains of northern Colorado. *J. Climate Appl. Meteor.*, **26,** 488–524.

Reinking, R. F., 1979: The onset and early growth of snow crystals by accretion of droplets. *J. Atmos. Sci.*, **36,** 870–881.

Reynolds, D. W., and A. S. Dennis, 1986: A review of the Sierra Cooperative Pilot Project. *Bull. Amer. Meteor. Soc.*, **67,** 513–523.

——, and A. P. Kuciauskas, 1988: Remote and in situ observations of Sierra Nevada winter mountain clouds: Relationships between mesoscale structure, precipitation and liquid water. *J. Climate Appl. Meteor.*, **27,** 140–156.

Sasyo, Y., 1971: Study of the formation of precipitation by aggregation of snow particles and the accretion of cloud droplets on snowflakes. *Pap. Meteor. Geophys.*, **22,** 69–142.

Vardiman, L., 1978: The generation of secondary ice particles by crystal–crystal collision. *J. Atmos. Sci.*, **35,** 2168–2180.

Warburton, J. A., and T. P. DeFelice, 1986: Oxygen isotopic composition of central Sierra Nevada precipitation. I. Identification of ice-phase water capture regions in winter storms. *Atmos. Res.*, **20,** 11–22.